Low-momentum interactions with Brown-Rho-Ericson scalings, and the density dependence of the nuclear symmetry energy

Huan Dong, T. T. S. Kuo, and R. Machleidt

Phys. Rev. C **83**, 054002 — Published 24 May 2011

DOI: 10.1103/PhysRevC.83.054002

Low-momentum interactions with Brown-Rho-Ericson scalings and the density dependence of the nuclear symmetry energy

Huan Dong and T. T. S. Kuo
Department of Physics and Astronomy, Stony Brook University, New York 11794-3800, USA

R. Machleidt
Department of Physics, University of Idaho, Moscow, Idaho 83844, USA

We have calculated the nuclear symmetry energy $E_{sym}(\rho)$ up to densities of $4 \sim 5\rho_0$ with the effects from the Brown-Rho (BR) and Ericson scalings for the in-medium mesons included. Using the V_{low-k} low-momentum interaction with and without such scalings, the equations of state (EOS) of symmetric and asymmetric nuclear matter have been calculated using a ring-diagarm formalism where the particle-particle-hole-hole ring diagrams are included to all orders. The EOS for symmetric nuclear matter and neutron matter obtained with linear BR scaling are both overly stiff compared with the empirical constraints of Danielewicz *et al.* [9]. In contrast, satisfactory results are obtained by either using the non-linear Ericson scaling or by adding a Skyrme-type three-nucleon force (TNF) to the unscaled V_{low-k} interaction. Our results for $E_{sym}(\rho)$ obtained with the non-linear Ericson scaling are in good agreement with the empirical values of Tsang *et al.* [7] and Li *et al.* [10], while those with TNF are slightly below these values. For densities below the nuclear saturation density ρ_0, the results of the above calculations are nearly equivalent to each other and all in satisfactory agreement with the empirical values.

PACS numbers: 21.65.Jk, 21.65.Mn, 13.75.Cs

I. INTRODUCTION

The nuclear matter symmetry energy is an important as well as very interesting subject in nuclear and astro-nuclear physics. As reviewed extensively in the literature [1–8], it plays a crucial role in determining many important nuclear properties, such as the neutron skin of nuclear systems, structure of nuclei near the drip line, and neutron stars' masses and radii. It is especially of importance that constraints on the nuclear matter equation of state (EOS) [9] and the density (ρ) dependence of the symmetry energy $E_{sym}(\rho)$ [7, 10] up to $\rho \simeq 4\rho_0$ have been experimentally extracted from heavy-ion collisions, ρ_0 being the saturation density of symmetric nuclear matter. There have been a large number of theoretical derivations of $E_{sym}(\rho)$ using, for example, the Brueckner Hartree-Fock (BHF) [11–13], Dirac BHF [6, 14–16], variational [17], relativistic mean field (RMF) [18] and Skyrme HF [19] many-body methods. The results of these theoretical investigations have exhibited, however, large variations for $E_{sym}(\rho)$. Depending on the interactions and many-body methods used, they can give either a 'hard' $E_{sym}(\rho)$, in the sense that it increases monotonically with ρ up to $\sim 5\rho_0$, or a 'soft' one where $E_{sym}(\rho)$ arises to a maximum value at $\rho \simeq 1.5\rho_0$ and then descends to zero at $\sim 3\rho_0$ [4, 8]. It appears that the predicted behavior of $E_{sym}(\rho)$ may depend importantly on the nucleon-nucleon (NN) interactions and the many-body methods employed.

In the present work, we shall calculate the nuclear symmetry energy using the low-momentum interaction V_{low-k} derived from realistic NN interactions V_{NN} using a renormalization group approach [20–24]. To our knowledge, this renormalized interaction has not yet been applied to the study of E_{sym}. As it is well known, most realistic V_{NN} contain hard cores, or strong short-range repulsions. This feature makes these interactions not suitable for being directly used in nuclear many-body calculations; they need to be 'tamed' beforehand. For many years, this taming is enacted by way of the BHF theory where V_{NN} is converted into the Brueckner G-matrix. A complication of the G-matrix is its energy dependence (see e.g. [25]), making it rather inconvenient for calculations. In the V_{low-k} approach, a different 'taming' procedure is employed; it is performed by 'integrating out' the high-momentum components of V_{NN} beyond a decimation scale Λ. In this way, the resulting V_{low-k} is energy independent. Furthermore V_{low-k} is nearly unique, namely the V_{low-k}s deduced from various realistic V_{NN} (such as [26–29]) are nearly identical to each other for decimation scale $\Lambda \simeq 2fm^{-1}$ [22, 23].

Using this V_{low-k} interaction, we shall first calculate the equations of state (EOS) $E(\rho, \alpha)$ for asymmetric nuclear matter, from which $E_{sym}(\rho)$ can be obtained. Here E is the ground-state energy per nucleon and ρ is the total baryon density. α is the isospin asymmetry parameter defined as $\alpha = (\rho_n - \rho_p)/\rho$, where ρ_n and ρ_p denote, repspectively, the neutron and proton density and $\rho = \rho_n + \rho_p$. Our EOS will be calculated using a ring-diagram many-body method [30–32]. As we shall discuss later, this method includes the particle-particle hole-hole ($pphh$) ring diagrams to all orders. In comparison, only the diagrams with two hole lines are included in the familiar HF, BHF and DBHF calculations. In other words, in these HF methods a closed Fermi sea is employed while in the ring-diagram framework the effects from the fluctuations of the Fermi sea are taken into account by including the $pphh$ ring diagrams to all orders.

The nuclear symmetry energy $E_{sym}(\rho)$ is related to the asymmetric nuclear matter EOS by

$$E(\rho,\alpha) = E(\rho,\alpha=0) + E_{sym}(\rho)\alpha^2 + O(\alpha^4). \quad (1)$$

The contributions from terms of higher order than α^2 are usually negligibly small, as illustrated by our results in section III. With such contributions neglected, we have

$$E_{sym}(\rho) = E(\rho,1) - E(\rho,0). \quad (2)$$

Then the symmetry energy is just given by the energy difference between neutron and symmetric nuclear matter. In calculating $E_{sym}(\rho)$, the above EOS clearly play an important role. In our calculation, we shall require that the NN interaction and many-body methods employed should give satisfactory results for $E(\rho,1)$ and $E(\rho,0)$ of, respectively, neutron and symmetric nuclear matter. The use of V_{low-k} alone, however, has not been able to reproduce the empirical nuclear saturation properties, the predicted saturation density and binding energy per particle being both too large compared with the empirical values of $\rho_0 \simeq 0.16\text{fm}^{-3}$ and $E \simeq -16$MeV for symmetric nuclear matter [30, 31]. To improve the situation, it may be necessary to include the effects from Brown-Rho (BR) scaling [35–37] for the in-medium mesons, or a three-nucleon force (TNF) [41]. BR scaling is suitable only for the low density region; it suggests that the masses of light vector mesons in medium are reduced 'linearly' with the density. We consider here the EOS up to about $\sim 5\rho_0$ and at such high density the linear BR scaling is clearly not applicable. In the present work we shall adopt the non-linear Ericson scaling [42] for the in-medium mesons and apply it to our $E_{sym}(\rho)$ calculations. The effects from the BR and Ericson scalings on the nuclear EOS and symmetry energy will be studied.

The organization of this paper is as follows. In section II we shall briefly describe our derivation of the low-momentum interaction V_{low-k} using a T-matrix equivalence approach. Some details about the calculation of the EOS for asymmetric nuclear matter from this interaction with the *pphh* ring diagrams summed to all orders will also be presented. Ericson scaling is a non-linear extension of linear BR scaling. The difference between them will be addressed in this section. Our results will be presented and discussed in section III. A summary and conclsion is contained in section IV.

II. FORMALISM

We shall calculate $E_{sym}(\rho)$ using a low-momentum ring-diagram approach [30–32], where the *pphh* ring diagrams are summed to all orders within a model space of decimation scale Λ. In this approach, we employ the low-momentum interaction V_{low-k} [20–24]. Briefly speaking, this interaction is obtained by solving the following T-matrix equivalence equations:

$$T(k',k,k^2) = V_{\rm NN}(k',k) + \frac{2}{\pi}\mathcal{P}\int_0^\infty \frac{V_{\rm NN}(k',q)T(q,k,k^2)}{k^2-q^2}q^2dq, \quad (3)$$

$$T_{\rm low-k}(k',k,k^2) = V_{\rm low-k}(k',k) + \frac{2}{\pi}\mathcal{P}\int_0^\Lambda \frac{V_{\rm low-k}(k',q)T_{\rm low-k}(q,k,k^2)}{k^2-q^2}q^2dq, \quad (4)$$

$$T(k',k,k^2) = T_{low-k}(k',k,k^2); (k',k) \le \Lambda. \quad (5)$$

In the above V_{NN} represents a realistic NN interaction such as the CDBonn potential [26]. $\mathcal{P}$ denotes principal-value integration and the intermediate state momentum q is integrated from 0 to ∞ for the whole-space T and from 0 to Λ for $T_{\rm low-k}$. The above V_{low-k} preserves the low-energy phase shifts (up to energy Λ^2) and the deuteron binding energy of V_{NN}. Since V_{low-k} is obtained by integrating out the high-momentum components of V_{NN}, it is a smooth 'tamed' potential which is suitable for being used directly in many-body calculations.

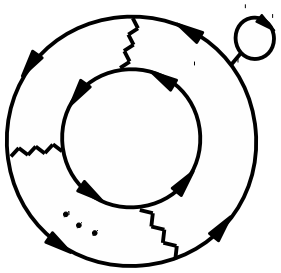

FIG. 1: Sample ring diagram included in the equation of state $E(\rho,\alpha)$. Each wave line represents a V_{low-k} vertex. The HF one-bubble insertions to the Fermion lines are included to all orders.

We use a ring-diagram method [30–32] to calculate the nuclear matter EOS. In this method, the ground-state energy is expressed as $E(\rho,\alpha) = E^{free}(\rho,\alpha) + \Delta E(\rho,\alpha)$ where E^{free} denotes the free (non-interacting) EOS and ΔE is the energy shift due to the NN interaction. In our ring-diagram approach, it is is given by the all-order sum of the *pphh* ring diagrams as illustrated in Fig. 1. Note that we include three types of ring diagrams, the proton-proton, neutron-neutron and proton-neutron ones. The proton and neutron Fermi momenta are, respectively, $k_{Fp} = (3\pi^2\rho_p)^{1/3}$ and $k_{Fn} = (3\pi^2\rho_n)^{1/3}$. With such ring diagrams summed to all orders, we have [31, 32]

$$\Delta E(\rho,\alpha) = \int_0^1 d\lambda \sum_m \sum_{ijkl<\Lambda} Y_m(ij,\lambda) \times Y_m^*(kl,\lambda)\langle ij|V_{\rm low-k}|kl\rangle, \quad (6)$$

where the transition amplitudes Y are obtaind from a *pphh* RPA equation [30–32]. Note that λ is a strength parameter, integrated from 0 to 1. The above ring-diagram method reduces to the usual HF method if only the first-order ring diagram is included. In this case, the above energy shift becomes $\Delta E(\rho,\alpha)_{HF} = \frac{1}{2}\sum n_i n_j \langle ij|V_{\rm low-k}|ij\rangle$ where n_k=(1,0) if $k(\leq,>)k_{Fp}$ for proton and n_k=(1,0) if $k(\leq,>)k_{Fn}$ for neutron.

The above V_{low-k} ring-diagram framework has been applied to nuclear matter [30] and neutron-star matter [31]. This framework has also been tested by applying it to dilute cold neutron matter at the limit that the $^1S_0$ scattering length of the underlying interaction approaches infinity [33, 34]. This limit is usually referred to as the unitary limit, and the corresponding potentials as unitarity potentials. For many-body systems at this limit, the ratio $\xi \equiv E_0/E_0^{free}$ is expected to be a universal constant of value ~ 0.44. (E_0 and E_0^{free} are, respectively, the interacting and non-interacting ground-state energies of the many-body system.) In previous calculations [33, 34] we have applied our ring-diagram method to calculate neutron matter using several very different unitarity potentials (a unitarity CDBonn potential obtained by tuning its meson parameters, and several square-well unitarity potentials). The ξ ratios given by our calculations for all these different unitarity potentials are all close to 0.44, in good agreement with the Quantum-Monte-Carlo results (see [34] and references quoted therein). In fact our ring-diagram results for ξ are significantly better than those given by HF and BHF. The above unitary calculations provide a stringent test for many-body methods, and our ring-diagram framework has done well in this test.

It is well known that the use of the free-space V_{NN} alone is not adequate for describing nuclear properties at high densities. To satisfactorily describe such properties, one may need to include the three-nucleon force [41] or the in-medium modifications to the nuclear interaction. In the present work, we shall employ in our EOS calculations nuclear interactions which contain the in-medium modifications suggested by the Brown-Rho (BR) [35, 36] and Ericson [42] scalings. These scalings are based on the relation [35, 36, 40] that hadron masses scale with the quark condensate $\langle\bar{q}q\rangle$ in medium as

$$\frac{m^*}{m} = \left(\frac{\langle\bar{q}q(\rho)\rangle}{\langle\bar{q}q(0)\rangle}\right)^{1/3} \tag{7}$$

where m^* is the hadron mass in a medium of density ρ, and m is that in free space. The quark condenstate $\langle\bar{q}q\rangle$ measures the chiral symmetry breaking, and its density dependence in the low-density limit is related [43, 44] to the free πN sigma term $\Sigma_{\pi N}$ by

$$\frac{\langle\bar{q}q(\rho)\rangle}{\langle\bar{q}q(0)\rangle} = 1 - \frac{\rho\Sigma_{\pi N}}{f_\pi^2 m_\pi^2} \tag{8}$$

where $f_\pi = 93$MeV is the pion decay constant and $\Sigma_{\pi N} = 45 \pm 7$MeV [45]. Applying the above scaling to mesons in low-density nuclear medium, one has the linear scaling [36]

$$\frac{m^*}{m} = 1 - C\frac{\rho}{\rho_0} \tag{9}$$

where m^* and m are, respectively, the in-medium and free meson mass, and C is a constant of value ~ 0.15. The above scaling will be referred to as the linear BR scaling. (Pions are not scaled because they are protected by chiral symmetry.) Nucleon-nucleon interactions are mediated by meson exchanges, and clearly the in-medium modifications of meson masses can significantly alter the NN interaction. These modifications could arise from the partial restoration of chiral symmetry at finite density/temperature or from traditional many-body effects. Particularly important are the vector mesons, for which there is now evidence from both theory [36, 46, 47] and experiment [48, 49] that the masses may decrease by approximately $10-15\%$ at normal nuclear matter density and zero temperature. It should be pointed out that, as reviewed recently by Hayano and Hatsuda [50] and Milov [51], there are also experiments which do not support the above in-medium decrease (or drop) of the meson mass. However, there are more experiments that support the in-medium decrease of meson masses as compared to experiments which do not see such evidence.[51] Density-dependent nuclear interactions obtained by applying the above scaling to the light mesons (ω, ρ and σ) which mediate the NN potential have been employed in studying the properties of nuclear matter [30, 31, 37, 38] and the $^{14}C \rightarrow ^{14}N$ β-decay [39].

We are interested in the EOS and E_{sym} up to densities as high as $\rho \simeq 5\rho_0$, and at such high densities the above linear scaling is clearly not suitable. How to scale the mesons in such high density region is still by and large uncertain. We shall adopt here the Ericson scaling [42] which is an extension of the BR scaling. In this scaling, a new relation for the quark condensate $\langle\bar{q}q\rangle$ based on chiral symmetry breaking is employed, namely

$$\frac{\langle\bar{q}q(\rho)\rangle}{\langle\bar{q}q(0)\rangle} = \frac{1}{1+\frac{\rho\Sigma_{\pi N}}{f_\pi^2 m_\pi^2}}. \tag{10}$$

Note that this relation agrees with the linear scaling relation of Eq.(8) for small ρ. The above scaling suggests a non-linear scaling for meson mass

$$\frac{m^*}{m} = \left(\frac{1}{1+D\frac{\rho}{\rho_0}}\right)^{1/3} \tag{11}$$

with $D = \frac{\rho_0\Sigma_{\pi N}}{f_\pi^2 m_\pi^2}$, and we shall refer to this scaling as the non-linear BR scaling. Using the empirical values for ($\Sigma_{\pi N}$, ρ_0, f_π, m_π), we have D= 0.35±0.06. In the present work, we shall employ the one-boson exchange BonnA potential [29] with its (ρ, ω, σ) mesons scaled using both the linear (Eq.(9)) and non-linear (Eq.(11)) BR scaling. This potential is chosen because it has a relatively simple structure which is convenient for scaling its meson parameters.

III. RESULTS AND DISCUSSIONS

Using both the unscaled and scaled BonnA potentials, we first calculate the ring-diagram EOS for symmetric nuclear matter to investigate if they can give saturation properties in good agreement with the empirical values. We employ the low-momentum interactions V_{low-k} from these potentials using a decimation $\Lambda = 3.0 fm^{-1}$, which is chosen because we are to study the EOS up to high densities of $\sim 5\rho_0$. As shown in Fig. 2, the EOS (labelled 'V_{low-k} alone') calculated with the unscaled potential saturates at $k_F \simeq 1.8 fm^{-1}$, which is too large compared with the empirical value, and it also overbinds nuclear matter. We then repeat the calculation including the medium modifications from the BR scalings. For the linear BR scaling (Eq.(9)), we have used C_ω=0.128, C_ρ=0.113 and C_σ=0.102. These parameters are chosen so as to have satisfactory saturation properties, namely they give $E_0/A \simeq$-15.5 MeV and $\rho_0 \simeq 0.17\ fm^{-3}$. In Fig. 2 we also present our results obtained with the non-linear BR scaling (Eq.(11)) using parameters $D_\omega = D_\rho$=0.40 and D_σ=0.30. They were chosen to provide satisfactory results for E_0/A and ρ_0.

We now discuss some boundary conditions associated with the BR scalings. With such scalings, the NN potential becomes $V_{NN}(\rho)$, namely it becomes density dependent. But it should satisfy certain boundary conditions: As ρ approaching zero, $V_{NN}(\rho)$ should become the free NN potential which reproduces the experimental NN scattering data and deuteron binding energy. This boundary condition is satisfied because we start from the realistic BonnA potential, and $V_{NN}(\rho = 0)$ is by construction the same as BonnA. In the present work, we also require the condition that $V_{NN}(\rho = \rho_o)$, ρ_o being the nuclear matter saturation density, reproduces the empirical nuclear matter saturation properties, by choosing the scaling parameters, the Cs or Ds, appropriately, as mentioned above. Thus, in our present work, we require $V_{NN}(\rho)$ to satisfy the above boundary conditions at ρ=0 and ρ_0. For densities in between and beyond, the density dependence of this potential is ruled by the scalings we employ.

It is of interest that for densities $\lesssim \rho_0$ the EOS given by the linear and non-linear BR scalings are practically equivalent to each other. As also seen from Fig. 2, the above equivalence begins to disappear for densities larger than ρ_0. There the EOS given by the linear BR scaling is much stiffer than that given by the non-linear one; the difference between them becomes larger and larger as density increases. In addition to the above two EOS, we have also calculated an EOS using the interaction given by the sum of the unscaled V_{low-k} and an empirical Skyrme three-nucleon force (TNF). The well-known emipirical Skyrme force [52] is of the form

$$V_{\rm Skyrme} = \sum_{i<j} V(i,j) + \sum_{i<j<k} V(i,j,k), \qquad (12)$$

where $V(i,j)$ is a two-nucleon momentum dependent interaction, and V(i,j,k) is a zero-range three-nucleon interaction which has played an indispensible role for nuclear saturation. For nucleons in a nuclear medium of density ρ, this three-nucleon force becomes a density-dependent two-nucleon force commonly written as

$$V_\rho(i,j) = \frac{t_3}{6}\rho\delta(\vec{r}_i - \vec{r}_j). \qquad (13)$$

In Fig. 2 the EOS labelled 'V_{low-k} with TNF' is obtained using the combined interaction of V_{low-k} (unscaled) and V_ρ. The parameter t_3 is adjusted so that the resulting EOS gives satisfactory saturation properties for symmetric nuclear matter. The EOS shown has t_3=2000 MeV-fm^6.

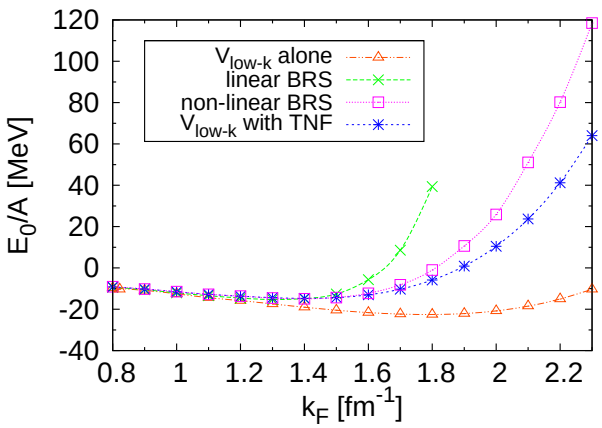

FIG. 2: Ring-diagram EOSs calculated for symmetric nuclear matter with different interactions. The BonnA interactions unscaled, scaled with the linear BR scaling of Eq. (9), and scaled with the non-linear scaling of Eq. (11) are used, respectively, for the results labelled 'V_{low-k} alone', 'linear BRS', and 'non-linear BRS'. For 'V_{low-k} with TNF' we use the unscaled BonnA interaction together with the Skyrme-type three-nucleon force of Eqs. (12-13).

It is of interest that the above three EOS (linear and non-linear BR, TNF) are nearly identical for densities $\lesssim \rho_0$, but they deviate from each other with increasing densities. Without experimental guidelines about the nuclear matter EOS above ρ_0, it would be difficult to determine which of these three EOS has the correct high density behavior. Fortunately, heavy-ion collision experiments conducted during the last several years have provided us with constraints of the EOS at high densities. Danielewicz *et al.* [9] have obtained a constraint on the EOS for symmetric nuclear matter of densities between $2\rho_0$ and $4.5\rho_0$, as shown by the red solid-line box in Fig. 3. Comparing our three EOSs with their constraint, the linear BRS EOS is clearly not consistent with the constraint and should be ruled out. This linear scaling is suitable for low densities, but definitely needs modification at high densities. It is primarily for this purpose that we have considered the non-linear scaling. As displayed in Fig. 3, the EOS with the non-linear BR scaling

is in much better agreement with the constraint than the linear-BR one. It satisfies the constraint well except being slightly above the constraint at densiies near $\sim 4.5\rho_0$. It is of interest that the EOS using V_{low-k} with the Skyrme-type TNF exhibits even better agreement with the constraint.

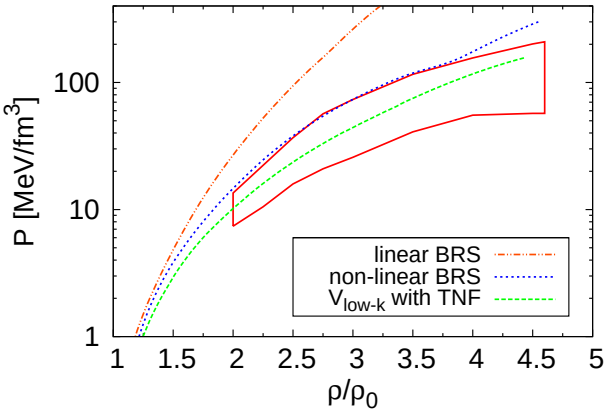

FIG. 3: The equations of state for symmetric nuclear matter calculated with different interactions as explained in the caption of Fig. 2. The Danielewicz constraint [9] derived from heavy-ion collisions is denoted by the 'solid-line box'.

So far we have studied the effects of the BR scalings and the TNF three-nucleon force on the EOS for symmetric nuclear matter. The neutron matter EOS is also an interesting and important topic [53, 54]. It plays a crucial role in determining the nuclear symmetry energies as well as the properties of neutron stars. It should be of interest to study also the effects of the above BR scalings and the TNF force on the EOS of neutron matter. Using the same V_{low-k} ring-diagram framework employed for symmetric nuclear matter and the same C, D and t_3 parameters, we have caculated the neutron matter EOS up to $4.5\rho_0$. Our calculated neutron-matter EOS are displayed in Fig. 4. Danielewicz *et al.* [9] have given two different constraints for the neutron matter EOS: a stiff one (upper solid-line box) and a soft one (lower solid-line box) which are both displayed in Fig. 4. As we can see, the linear BRS EOS is again producing too much pressure. The non-linear BRS EOS agrees well with the stiff constraint (upper box) while the TNF EOS is fully within the soft constraint box. To further test these two EOS (non-linear BRS and TNF), it would be very helpful to have narrower experimental constraints on the neutron matter EOS.

The symmetry energy E_{sym} is a topic of much current interest, and extensive studies have been carried out to extract its density dependence from heavy-ion collision experiments [7, 10]. Based on such experiments, Li *et al.* [10] suggested an empirical relation

$$E_{sym}(\rho) \approx 31.6(\rho/\rho_0)^{\gamma};\ \gamma = 0.69 - 1.1, \qquad (14)$$

for constraining the density dependence of the symmetry energy. Also based on such experiments, Tsang *et al.* [7] recently proposed a new empirical relation for the symmetry energy, namely

$$E_{sym}(\rho) = \frac{C_{s,k}}{2}\left(\frac{\rho}{\rho_0}\right)^{2/3} + \frac{C_{s,p}}{2}\left(\frac{\rho}{\rho_0}\right)^{\gamma_i} \qquad (15)$$

where $C_{s,k} = 25$MeV, $C_{s,p} = 35.2$MeV and $\gamma_i \approx 0.7$. It should be useful and of interest to check if our calculated $E_{sym}(\rho)$ is consistent with the above relations.

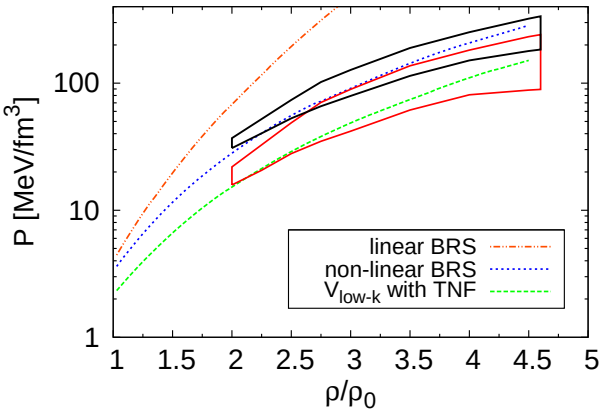

FIG. 4: The equations of state for neutron matter calculated with different interactions as explained in the caption of Fig. 2. The Danielewicz constraint [9] derived from heavy-ion collisions is denoted by the 'solid-line box'. See text for more explanations.

Using the ring-diagram framework described earlier, we have calculated the ground-state energy $E(\rho, \alpha)$ for asymmetric nuclear matter. (Recall that the asymmetry parameter is $\alpha = (\rho_n - \rho_p)/\rho$.) Some representative results are shown in Fig. 5: the results in the left panel are obtained with the 'V_{low-k} with TNF' interaction while for the right panel the 'non-linear BR' interaction is used. As seen, $E(\rho, \alpha)$ varies with α^2 almost perfectly linearly, for a wide range of ρ. (Note that in Fig. 5 we plot the energy difference $E_{sym}(\rho, \alpha) - E_{sym}(\rho, 0)$.) This is a desirable result, indicating that our ring-diagram symmetry energy can be accurately obtained from the simple relation given by Eq. (2), namely the energy difference between neutron and symmetric nuclear matter. Note that the above linear behavior has also been observed in previous symmetry energy calculations using different many-body methods [4, 55].

In Fig. 6, the 'shaded area' represents the empirical constraint, Eq.(14), of Li *et al.* [10]. As seen, there are large uncertainties in the high-density region. The empirical relation Eq.(15) of Tsang *et al.* [7] is given by the 'second curve from bottom' in the figure. As seen, the density dependence of this relation is slightly below the softest limit (lower boundary of the shaded area) of Eq.(14). Our 'non-linear BR' results are in the middle of the shaded area, in good agreement with the empirical constraint of [10]. Our results with the TNF force are

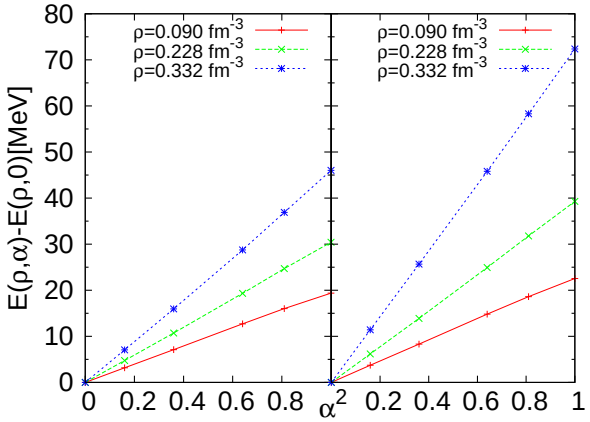

FIG. 5: Ring-diagarm equations of state of asymmetric nuclear matter. See text for more explanations.

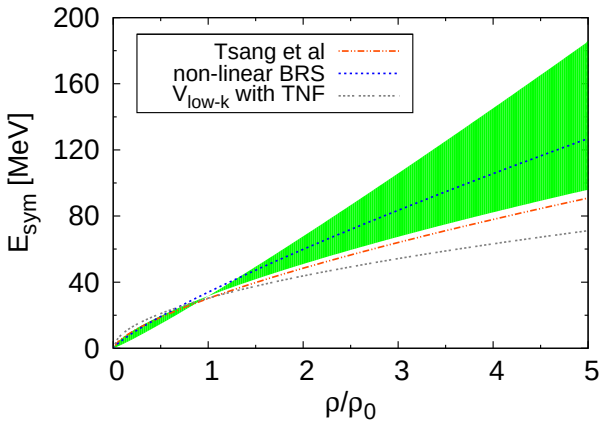

FIG. 6: The density dependence of symmetry energies calculated with different interactions as explained in the caption of Fig.2. The empirical results of Tsang et al. (dot-dash line) and Li et al. (shaded area) are from [7] and [10], respectively.

below the empirical ones of both [10] and [7], giving a softer density dependence than both. It may be noticed that for densities ($\rho \lesssim \rho_0$), the calculated and empirical results are all in good agreement with each other. The symmetry energies given by them at ρ_0 are all close to $\sim$ 30MeV, which is also the only well determined empirical value. Furthermore, our calculated symmetry energies all increase monotonically with density. We have required our nuclear matter EOS to satisfy certain empirical constraints, and with such requirements it may be difficult for our present calculations to have a soft $E_{sym}(\rho)$ as soft as the supersoft one of [8] which saturates at density near $\sim 1.5\rho_0$.

We have found that our symmetry energies can be well fitted by expressions of the same forms as Eqs.(14) and (15), with the exponents γ and γ_i treated as parameters. In Table I, we compare the exponents determined from our results with the empirical ones of [10] and [7]. The γ exponent given by the non-linear BR scaling is in good agreement with the empirical values of [10]. The empirical γ_i of [7] is, however, about half-way between the γ_i obtained with 'non-linear BRS' and that with 'TNF'.

TABLE I: Density exponents for the nuclear symmetry energy $E_{sym}(\rho)$ calculated with different interactions as explained in the caption of Fig. 2. The exponents γ and γ_i are defined respectively in Eqs. (14) and (15).

	γ	γ_i
Li *et al.* [10]	0.69-1.1	
Tsang *et al.* [7]		0.7
non-linear BRS	0.82	1.04
V_{low-k} with TNF	0.53	0.43

IV. SUMMARY AND CONCLUSION

Employing the V_{low-k} low-momentum interactions, we have calculated the nuclear symmetry energy $E_{sym}(\rho)$ up to a density of $\sim 5\rho_0$ using a ring-diagram framework where *pphh* ring diagrams are summed to all orders. We first calculate the EOS for symmetric nuclear matter and neutron matter and compare our results with the corresponding empirical constraints of Danielewicz *et al.* [9]. To have satisfactory agreements with such constraints, we have found it necessary to include certain medium corrections to the free-space NN interations. In other words, the effective NN interactions in medium are different from those in free space, and when using them in nuclear many-body problems it may be necessary to include the renormalization effects due to the presence of other nucleons. We have considered several methods to incorporate such medium corrections. Although the nuclear matter saturation properties can satisfactorily be reproduced by including the medium corrections from the well-known linear Brown-Rho scaling for the in-medium mesons, this scaling produces an EOS which is too stiff compared with the Danielewicz constraints. We have found that the EOS obtained with the Ericson non-linear scaling (referred to earlier as the non-linear BR scaling) are in good agreement with the Danielewicz constraints. We have considered another method to render the effective interaction density dependent, namely adding a Skyrme-type three-nucleon force (TNF) to the unscaled V_{low-k} interaction. The EOS so obtained are also in good agreement with the Danielewicz constraints, but the resulting neutron matter EOS is significantly softer than that with the non-linear scaling. The three methods (linear and non-linear scalings, and TNF) all have reproduced well the empirical saturation properties of nuclear matter ($\rho_0 \approx 0.17\text{fm}^{-3}$ and $E_0/A \approx -15$MeV), but their results at high densities are different. We have determined the scaling parameters C (linear BR scaling) and D (non-linear Ericson scaling) by fitting the above saturation properties. It is encouraging that the results, ($0.102 \lesssim C \lesssim 0.128$) and ($0.30 \lesssim D \lesssim 0.40$), so obtained

are actually in good agreement with the theoretical result $D \simeq 0.35 \pm 0.06 \simeq 3C$ given by Eqs.(7-11).

Including the above medium modifications, we proceed to calculate the nuclear symmetry energies. We have found that the $E_{sym}(\rho, \alpha)$ given by our asymmetric ring-diagram calculations depends on α^2 almost perfectly linearly. This is a rather useful result, suggesting that the symmetry energy as calculated by our ring-diagram method can be reliably obtained from the simple energy difference between symmetric nuclear matter and neutron matter. Our symmetry energies obtained with the non-linear Ericson scaling agree well with the empirical constraints of [10], and are slightly above the empirical values of [7]. Our results with the TNF force is slightly below the empirical results of both [10] and [7]. The non-linear Ericson scaling has given satisfactory results for the equations of states of nuclear matter and nuclear symmetry energies up to a density of $\sim 5\rho_0$. We believe this scaling provides a suitable extension of the linear BR scaling to moderately high densities of $\lesssim 5\rho_0$. Our calculated $E_{sym}(\rho)$ all increase monotonically with ρ up to $\sim 5\rho_0$. It may be of interest to carry out further studies about the possibility of obtaining a supersoft symmetry energy which may saturate at some low density of $\sim 1.5\rho_0$ [8].

Acknowledgement We thank Professor Danielwicz for sending us the experimental data, and G.E. Brown and E. Shuryak for many helpful discussions. This work is supported in part by the U.S. Department of Energy under Grant Nos. DE-FG02-88ER40388 and DE-FG02-03ER41270 (R.M.), and the U.S. National Science Foundation under Grant No. PHY-0099444.

[1] V. Baran *et al.*, Phys. Rep. **410**, 335(2005).
[2] A. W. Steiner, M. Prakash, J. Lattimer and P.J. Ellis, Phys. Rep. **411**, 325(2005).
[3] J. M. Lattimer and M. Prakash, Phys. Rep. **442**, 109(2007).
[4] B. A. Li, L. W. Chen and C. M. Ko, Phys. Rep. **464**, 113 (2008).
[5] M. Di Toro et al., Prog. Part. Nucl. Phys. **62**, 383 (2008).
[6] F. Sammarruca, Int. J. Mod. Phys. E **19**, 1259 (2010); arXiv:1002.0146 [nucl-th].
[7] M.B. Tsang, Yingxun Zhang, P. Danielewicz, M. Famiano, Zhuxia Li, W.G. Lynch and A.W. Steiner, Phys. Rev. Lett. **102**, 122701(2009).
[8] Z. Xiao, B.A. Li, L.W. Chen, G.C. Yong and M. Zhang Phy. Rev. Lett. **102**, 062502 (2009).
[9] P. Danielewicz, R. Lacey and W. G. Lynch, Science **298**, 1592 (2002).
[10] B.A. Li and L.W. Chen, Phys. Rev. **C72**,064611(2005).
[11] I. Bombaci and U. Lombardo, Phys. Rev. **C44**, 1892 (1991).
[12] W.Zuo, A. Leguene, U. Lombardo, and J. F. Mathiot, Eur. Phys. J. **A14**, 469(2002).
[13] Z. H. Li *et al.*, Phys. Rev. **C74**, 047304(2006).
[14] D. Alonso and F. Sammarruca, Phys. Rev. C **67**, 054301 (2003).
[15] P.G. Krastev and F. Sammarruca, Phys. Rev. **C74**, 025808 (2006).
[16] E.N.E. van Dalen, C. Fuchs and A. Faessler, Eur. Phys. J. **A31**, 29(2007).
[17] R.B. Wiringa,V. Fiks, A. Fabrocini, Phys. Rev. **C38**, 1010(1988).
[18] L.W. Chen, C.M. Ko, B.A. Li, Phys. Rev. **C76**, 054316(2007).
[19] L. W. Chen, C. M. Ko and B. A. Li, Phys. Rev. Lett. **94**, 032701(2005).
[20] S.K. Bogner, T.T.S. Kuo, L. Coraggio, A. Covello, Nucl. Phys. **A684**, 432(2001)
[21] S.K. Bogner, T.T.S. Kuo, L. Coraggio, A. Covello and N. Itaco, Phys. Rev. C**65**, 051301(R)(2002)
[22] S.K. Bogner, T.T.S.Kuo and A. Schwenk, Phys. Rep. **386**,1 (2003)
[23] S.K. Bogner, T.T.S.Kuo, A. Schwenk, D. R. Entem and R. Machleidt, Phys. Lett. **B576**, 265(2003).
[24] J. D. Holt, T. T. S. Kuo and G. E. Brown, Phys. Rev. C **69** (2004) 034329.
[25] T.T.S. Kuo, Z. Y. Ma and R. Vinh Mau, Phys. Rev. **33**, 717(1986).
[26] R. Machleidt, Phys. Rev. C **63** 024001 (2001).
[27] V.G.J. Stoks, R.A.M. Klomp, C.P.F. Terheggen and J.J. de Swart, Phys. Rev. C **49**, 2950 (1994).
[28] R. B. Wiringa, V.G.J. Stoks and R. Schiavilla, Phys. Rev. C **51**, 38 (1995).
[29] R. Machleidt, Adv. Nucl. Phys. **19**, 189-376 (1989).
[30] L. W. Siu, J. W. Holt, T. T. S. Kuo and G. E. Brown, Phys. Rev. **79**, 0540004 (2009)
[31] H. Dong, T.T.S. Kuo and R. Machleidt, Phys. Rev. C **80**, 065803(2009).
[32] H. Q. Song, S. D. Yang and T. T. S. Kuo, Nucl. Phys. **A462** (1987) 491.
[33] L. W. Siu, T.T.S. Kuo and R. Machleidt, Phys. Rev. C **77**, 034001(2008).
[34] H. Dong, L.W. Siu, T.T.S. Kuo and R. Machleidt, Phys. Rev. C **81**, 034003(2010).
[35] G.E. Brown and M. Rho, Phys. Rev. Lett. **66**, 2720(1991).
[36] T. Hatsuda and S.H. Lee, Phys. Rev. C **46**, R34(1992).
[37] R. Rapp, R. Machleidt, J.W. Durso and G.E. Brown, Phys. Rev. Lett. **82**, 1827(1999).
[38] J.W. Holt, G.E. Brown, Jason D. Holt and T.T.S. Kuo, Nucl. Phys. **A785**, 322(2007).
[39] J.W. Holt, G.E. Brown, T.T.S. Kuo, J.D. Holt and R. Machleidt, Phys.Rev. Lett. **100**, 062501(2008).
[40] Y. Nambu and G. Jona-Lasino, Phys. Rev. **122**, 345(1961).
[41] S. K. Bogner, A. Schwenk, R. J. Furnstahl and A. Nogga, Nucl. Phys. **A763** (2005) 59.
[42] M. Ericson, Phys. Lett. B **301**,11(1993)
[43] T.D. Cohen, R.J. Furnstahl, D.K. Griegel, Phys. Rev. C**45**,1881(1992).
[44] M. Lutz, S. Klimt, W. Weise, Nucl. Phys. A**542**,521(1992).
[45] J. Gasser, H. Leutwyler and M.E. Sainio, Phys. Lett. B **253**,252(1991).
[46] M. Harada and K. Yamawaki, Phys. Rept. **381** (2003) 1.
[47] F. Klingl, N. Kaiser, and W. Weise, Nucl. Phys. **A624** (1997) 527.
[48] D. Trnka *et al.*, Phys. Rev. Lett. **94** (2005) 192303.
[49] M. Naruki *et al.* Phys. Rev. Lett. **96** (2006) 092301.
[50] R. S. Hayano and T. Hatsuda, Rev. Mod. Phys. **82**, 2949(2010).
[51] A. Milov, Eur. Phys. Jour. **C61** , 741(2009).
[52] P. Ring and P. Schuck, *The Nuclear Many-Body Problem* (Springer-Verlag, New York, 1980), and references quoted therein.
[53] B. Friedman and V. R. Pandaripande, Nucl. Phys. **A361**, 502(1981)
[54] B. A. Brown, Phys. Rev. Lett. **85**, 5296 (2000).
[55] Lagaris and V.J. Pandharipande, Nucl. Phys. **A369**, 470(1981).